Holocene sedimentology and coastal geomorphology of Zakynthos Island, Ionian Sea: A history of a divided Mediterranean island

Article *in* Palaeogeography Palaeoclimatology Palaeoecology · September 2017

DOI: 10.1016/j.palaeo.2017.09.018

CITATIONS
3

READS
390

6 authors, including:

Pavlos Avramidis
University of Patras
70 PUBLICATIONS **483** CITATIONS
SEE PROFILE

George Iliopoulos
University of Patras
63 PUBLICATIONS **336** CITATIONS
SEE PROFILE

Kostas Nikolaou
University of Patras
9 PUBLICATIONS **30** CITATIONS
SEE PROFILE

Andreas Koutsodendris
Universität Heidelberg
43 PUBLICATIONS **457** CITATIONS
SEE PROFILE

Palaeogeography, Palaeoclimatology, Palaeoecology 487 (2017) 340–354

Contents lists available at ScienceDirect

Palaeogeography, Palaeoclimatology, Palaeoecology

journal homepage: www.elsevier.com/locate/palaeo

Holocene sedimentology and coastal geomorphology of Zakynthos Island, Ionian Sea: A history of a divided Mediterranean island

Pavlos Avramidis[a,*], George Iliopoulos[a], Konstantinos Nikolaou[a], Nikolaos Kontopoulos[a], Andreas Koutsodendris[b], Gert Jan van Wijngaarden[c]

[a] Department of Geology, University of Patras, 26504 Rio, Patras, Greece
[b] Paleoenvironmental Dynamics Group, Institute of Earth Sciences, University of Heidelberg, Im Neuenheimer Feld 234, D-69120 Heidelberg, Germany
[c] Amsterdam Centre for Ancient Studies and Archaeology, University of Amsterdam, Turfdraagsterpad 9, 1012 XT Amsterdam, The Netherlands

ARTICLE INFO

Keywords:
Palaeoenvironment
Sediments
Landscape archaeology
Coastal changes
Vasilikos peninsula
Brackish
Fresh water

ABSTRACT

The island of Zakynthos is one of the most seismically active areas in the Mediterranean region because it is located very close to the convergent boundary between the African and Eurasian plates. Its evolution during the Holocene has been influenced by tectonic activity, catastrophic events and relative sea level changes. The scope of the present paper is to examine the Holocene palaeoenvironmental changes of the coastal areas of Zakynthos Island using a multidisciplinary approach, combining sedimentological and palaeontological data with ^{14}C and OSL dating from four cores of a maximum depth of ~30 m. The integrated results reveal that sea level and tectonic activity have brought significant modifications in the coastal geomorphic settings of the island during the past ~10,000 yr B.P. The depositional environments and the palaeontological biofacies document four main geomorphological evolutionary stages of the island. We identified fully marine and lagoonal deposits with marine influence (before 4100 yr B.P.), as well as brackish and freshwater limnic depositional environments (around 4100 yr B.P. to present). The interpretation of our data indicates that Zakynthos island was separated into two main parts before the middle Neolithic period (around 7500 yr B.P.) with Vasilikos peninsula in the SE being isolated from the main island. The fact that Zakynthos Island was a divided Mediterranean island for a significant period of time in its prehistory is of great importance to understand better the archaeological landscapes of Zakynthos and the other Ionian Islands.

1. Introduction

Coastal areas and adjacent continental shelves constitute dynamic depositional environments, which are shaped by the interaction of tectonic activity, sea level change and diverse environmental factors related to human activities (Kraft et al., 1977; Anthony et al., 2014). This holds particularly true for the Mediterranean region for which morphotectonic evolution, climatic change and sea level rise have shaped out a highly diversified coastal geomorphology during the Holocene (Anthony et al., 2014). Coastal palaeoenvironmental changes in the Mediterranean region during the Holocene are, in turn, a fundamental parameter that influences present and past societies (Rapp and Kraft, 1994; Aberg and Lewis, 2000; Weiberg et al., 2016). Early Mediterranean civilizations made ample use of the coastal areas and islands of the central and eastern Mediterranean, as inferred from the wide distribution of the Phoenician, Greek and Roman settlements (Davis and Fitzgerald, 2004). The Balkan Peninsula, and particularly Greece, has hosted human societies for > 6000 years (Fouache et al., 2010). Several studies have documented coastal palaeoenvironmental changes in specific locations in Greece during the Holocene, demonstrating the role of factors such as relative sea-level changes, tectonic activity, catastrophic events (floods, tsunami, etc.), sediment budget and river deltas progradation (Vött, 2007; Marriner and Morhange, 2007; Evelpidou et al., 2010; Brückner et al., 2010; Ghilardi et al., 2012; Ghillardi et al., 2013; Pavlopoulos et al., 2013; Apostolopoulos et al., 2014; Papadopoulos et al., 2014; Avramidis et al., 2014; Anthony et al., 2014; Weiberg et al., 2016), In this study, we examine the role of such processes in the coastal geomorphological evolution of the island of Zakynthos, contributing to the better understanding of the coastal geomorphology and archaeological landscape of the island.

In the eastern Mediterranean region coastal areas and lagoons constitute important archives for the study of Holocene palaeoenvironmental changes. Several proxies have been employed to reconstruct shoreline dislocation, sea level and palaeoclimatic changes during the

* Corresponding author at: University of Patras, Department of Geology, Division of General Marine Geology and Geodynamics, 26504 Rio, Patras, Greece.
E-mail address: p.avramidis@upatras.gr (P. Avramidis).

http://dx.doi.org/10.1016/j.palaeo.2017.09.018
Received 17 May 2017; Received in revised form 7 September 2017; Accepted 17 September 2017
Available online 21 September 2017
0031-0182/

Holocene, including sedimentological, palaeontological, geochemical and archaeological methods (e.g., Fouache and Pavlopoulos, 2005; Vött, 2007; Brückner et al., 2010; Finné et al., 2011; Pavlopoulos et al., 2012; Haenssler et al., 2013; Weiberg et al., 2016). Sea-level rise is one of the principal processes that affected the geomorphology and coastal depositional environments of the Mediterranean region during the Holocene. As the result of the sea level rise, the consequent marine transgression inundated lowlands forming coastal lagoons, marshes and embayments. Moreover, the convergent boundary of Eurasian and African plates lies within the eastern Mediterranean and is one of the most seismically active regions worldwide. As a consequence of the high seismo-tectonic activity, coastal areas have been influenced by marine incursions due to tsunamis (Kontopoulos and Avramidis, 2003; Avramidis et al., 2013; Vött and Kelletat, 2015). For the Holocene there are several geoarchaeological findings that point to tsunami events all around the eastern Mediterranean Sea (Papadopoulos et al., 2014) and particularly in western and southern Greece (Vött et al., 2009, 2011; Kontopoulos and Avramidis, 2003; Scheffers et al., 2008; Bruins et al., 2008; Vött and Kelletat, 2015).

The goal of the present paper is to reconstruct the Holocene coastal palaeoenvironmental changes of Zakynthos Island, western Greece using multiproxy sedimentological, palaeontological and chronological data. For the purpose of the study, sedimentological, micro- and macropalaentological as well as geochemical methods were applied on two ~30-m-long cores, for which age models were constrained by ^{14}C and optically stimulated luminescence (OSL) dating. Our results were paired with available data from two previous studies on Zakynthos, i.e., Alykes lagoon (Avramidis et al., 2013) and Lake Keri (Papazisimou et al., 2000), to better understand the coastal evolution of the island during the Holocene.

2. Study area

Western Greece, including the Ionian Islands and Zakynthos Island, is one of the most seismically active regions in Mediterranean Sea (Papazachos and Papazachou, 1997) (Fig. 1A,B). The Ionian Islands occupy a key position in the central and eastern Mediterranean for their geotectonic framework, as they are part of a multiple junction region with different types of plate boundaries (Accordi et al., 2014) and underwent clockwise rotation, from the Palaeocene, for a total of 45–50° (Kissel et al., 1985; van Hinsbergen et al., 2005). Sedimentological and geomorphological studies conducted along the western Peloponnese and Ionian islands indicated the existence of several tsunamigenic events that took place during the Holocene (Avramidis et al., 2013; Vött and Kelletat, 2015). Zakynthos island is located very close to the convergent boundary between African and Eurasian plates (Fig. 1A) and is undergoing very rapid and intense ground deformations (around 50 mm/yr) (Lagios et al., 2007). The island has a complex palaeogeographic history as the result of the westward migration of external Hellenides, which played the key role for the syn- and post collisional phases (Underhill, 1989; Papanikolaou et al., 2011; Kokkalas et al., 2012; Karakitsios, 2013). The sedimentation in Zakynthos Island is characterized by the deposition of evaporites and calcareous rocks of Triassic to Miocene age and by the clastic deposits of Pliocene-Quaternary age (Fig. 2). Both compressional and extensional tectonism influenced the geomorphology and the sedimentation of the island (Zelilidis et al., 1998).

The study area covers the coastal areas of the northeastern and southern parts of the island, including Alykes lagoon, former Lake Makri now drained and located at today's airport area, and Keri Lake that has been known since ancient times as 'Herodotus springs' (Fig. 2). For the present study. Data from four cores have been evaluated including: (a) a 21-m-depth borehole from Alykes Lagoon (Avramidis et al., 2013); (b) two 30-m-depth boreholes from former lake Makri (this study); and (c) a 7-m-depth borehole (Papazisimou et al., 2000; Avramidis et al., 2017) from Keri Lake.

3. Material and methods

3.1. Sediment cores

For the present study data from two new cores (G-1: 37°45′27.22″ N, 20°53′20.23″ E and G-2: 37°44′37.44″ N, 20°52′40.32″ E), up to a maximum depth of 30 m, were drilled in the central and southern part of the island, near the Zakynthos airport, on the site of former Lake Makri. Geographical positions and elevations of the cores were determined with a differential GPS ProMark 3 Magellan. In addition, we have re-evaluated existing data from two cores that were drilled in the northern eastern part of the island in Alykes lagoon (Core GA-1; 37°50′32″ N, 20°45′51″ E; Avramidis et al., 2013) and in the southern part in Keri Lake (Core KZ; 37°41′07″ N, E 20°49′46″ E; Papazisimou et al., 2000; Avramidis et al., 2017) (Fig. 2). Cores GA-1, G-1 and G-2

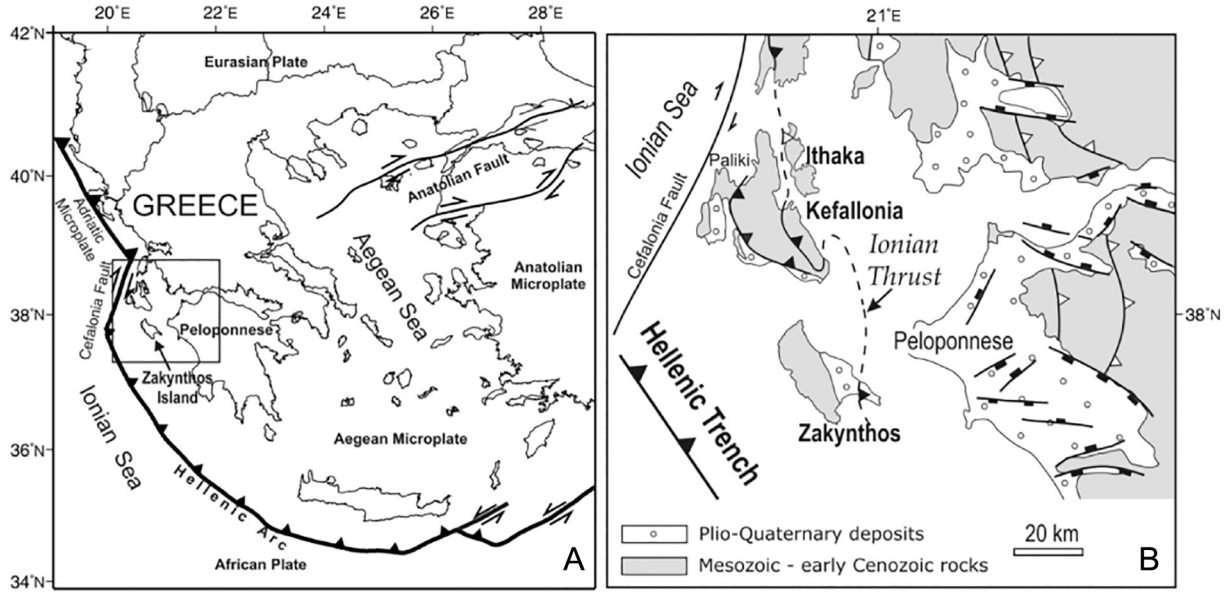

Fig. 1. (A) Simplified map of Greece showing the Hellenic trench, the major fault systems and the study area Zakynthos Island and (B) map of western Greece with the main fault systems and the Ionian Island Zakynthos, Kefalonia and Lefkada.

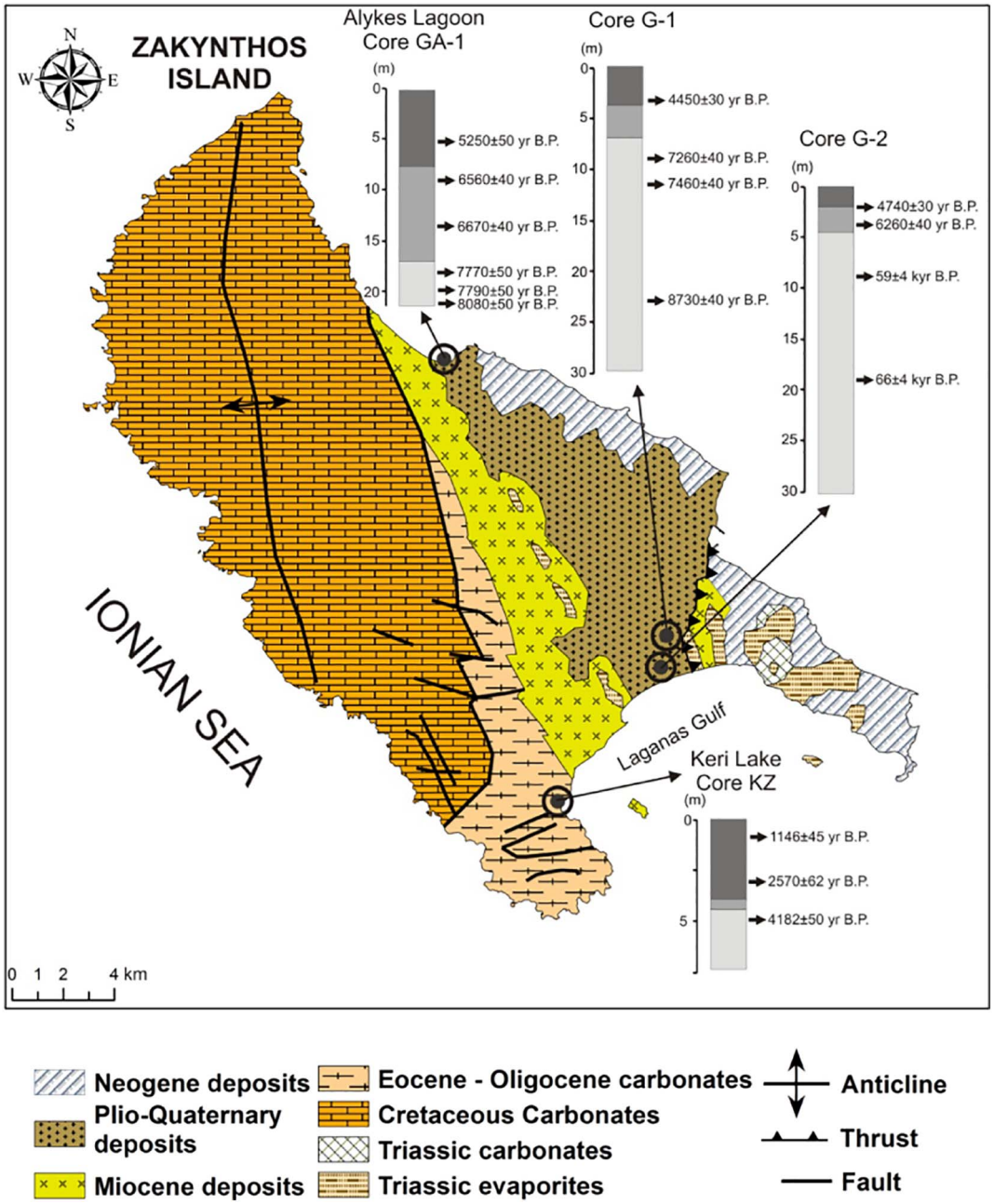

Fig. 2. Geological map of Zakynthos Island with the main tectonic structures and the borehole locations (I.G.M.E., 1980). Lithological units for each core are indicated with different colours. Core data from Alykes Lagoon and Keri Lake have been adapted from Avramidis et al. (2013) and Papazisimou et al. (2000), Avramidis et al. (2017), respectively.

were drilled using a rotation Longyear 38, with single tube core barrel with tungsten carbide bit and 101 mm diameter; whereas Core KZ was drilled by an Eijkelkamp vibrating corer with open window barrel tubes. All extracted samples of the cores were sealed with cling film and transported in wooden boxes for further analysis at the University of Patras. Sediment types, structures, colour, as well as contact depths and bed characteristics, were recorded. The location of each core, the total drilling depth and the available dating data are shown in Fig. 2 and Tables 1 and 2.

3.2. Sedimentology

Standard sedimentological analyses were carried out on 206 samples including grain size analysis, total organic carbon (TOC), total nitrogen (TN) (DIN EN 15936, 2009) and calcium carbonate content ($CaCO_3$). Sediment classification was based on grain size analysis and based on Folk (1974) nomenclature. Material coarser than 4 Φ was dry sieved, while fine grained material > 4 Φ was analyzed with a Malvern Mastersizer 2000, and finally grain size distributions were calculated. Grain size statistical parameters such as mean, sorting, skewness and kurtosis were calculated using GRADISTAT v.4 software (Blott and Pye, 2001). Colours were identified using a Minolta CM-2002 handheld spectrophotometer based on the Munsell colour chart.

In addition, TOC and TN were measured using a Shimadzu TOC-VCSH TOC/TN analyzer coupled to a chemiluminescence detector (TNM-1 TN unit), creating a simultaneous analysis system. Oxidative combustion – infrared analysis was used for TOC based on DIN EN 15936 and oxidative combustion-chemiluminescence method for TN based on ASTM D5176 (Bekiari and Avramidis, 2014). $CaCO_3$ content (%) was calculated using a FOG II/Digital hand-held soil calcimeter Version 2/2014 (BD INVENTIONS). $CaCO_3$ (%) calculation was based on measuring emitted CO_2 a modification of the method by Müller and

Table 1
List of radiocarbon dates used for the age depth models of the four cores, i.e., G-1, G-2, KZ and GA-1.

Sample	Laboratory Reference	Depth (m)	Material Dated	Conventional age ^{14}C yr B.P.	Reference
CORE G-1 (former Lake Makri)					
G1-R-1	Beta - 319,344	4.14	*Cerastoderma* valve	4450 ± 30	This study
G1-R-6	Beta - 319,346	8.7	*Cerastoderma* valve	7260 ± 40	This study
G1-R-9	Beta - 319,345	11.56	*Cerastoderma* valve	7460 ± 40	This study
G1-R-10	Beta - 319,347	23.7	*Cerastoderma* valve	8730 ± 40	This study
CORE G-2 (former Lake Makri)					
G-2-R-1	Beta - 319,348	2,54	*Cerastoderma* valve	4740 ± 30	This study
G-2-R-2	Beta - 319,349	3,86	*Cerastoderma* valve	6260 ± 40	This study
CORE KZ (Keri Lake)					
KZ-7a	DEM-806	0.92	Organic material	1146 ± 45 BP	Papazisimou et al. (2000) Avramidis et al. (2017)
KZ-7b	DEM-807	2.77	Organic material	2570 ± 62 BP	Papazisimou et al. (2000) Avramidis et al. (2017)
KZ-7c	DEM-808	4.67	Organic material	4182 ± 50 BP	Papazisimou et al. (2000) Avramidis et al. (2017)
CORE GA-1 (Alykes)					
R-2	Beta - 246,906	5.75	*Cerastoderma* valve	5250 ± 50	Avramidis et al. (2013)
R-4	Beta - 252,827	8.42	*Cerastoderma* valve	6560 ± 40	Avramidis et al. (2013)
R-6	Beta - 254,018	11.9	*Cerastoderma* valve	6670 ± 50	Avramidis et al. (2013)
R-11	Beta - 252,828	13.9	*Cerastoderma* valve	6720 ± 40	Avramidis et al. (2013)
R-18	Beta - 254,019	18.8	*Cerastoderma* valve	7770 ± 50	Avramidis et al. (2013)
R-20	Beta - 246,907	20.0	*Cerastoderma* valve	7790 ± 50	Avramidis et al. (2013)
R-21	Beta - 254,020	21.2	*Cerastoderma* valve	8080 ± 50	Avramidis et al. (2013)

Table 2
Dates based on optical stimulated luminescence (OSL) data from core G-2.

Sample	Depth (m)	Equivalent dose (DE), Gy	Dose rate (d), mGy/a	Standard deviation (σ)	Coefficient of variation (v), %	Age (kyr B.P.)
G2OSL1	8.40–8.60	193.2	3.29 ± 0.26	13.8	7.1	58.7 ± 6.2
G2OSL2	18.30–18.45	186.1	2.82 ± 0.23	6.3	3.4	65.9 ± 5.8

Gastner (1971) and Jones and Kaiteris (1983).

3.3. Chronology

The chronological framework of our study is based on sixteen (16) radiocarbon age determinations (Table 1) and two (2) optically stimulated luminescence (OSL) dates (Table 2). Radiocarbon analyses were made at Beta Analytic (Miami, USA) and the National Center of Scientific Research (N.C.S.R. – Democritus, Athens Greece), while the OSL dating was carried out in N.C.S.R. – Democritus. Results such as conventional radiocarbon age and two-sigma calendar calibration were taken. Based on the radiocarbon dates, the age-depth-models for all cores were calculated based on Bayesian statistics using OxCal (version 4.1) calibration software (Bronk Ramsey, 2009) and taking into account the IntCal13 calibration curve (Reimer et al., 2013). For each run, a k-value of 150 was used, which gives 7 mm calculation increment. For the shell samples used for ^{14}C analysis (Table 1) a reservoir correction of 390 ± 85 yr, which is typical for marine/brackish environments, was applied (Siani et al., 2000). All selected dated shells were whole and very well preserved without erosional traces. The OSL samples were submitted for standard chemical and mechanical isolation of quartz. Initial steps included use of HCl (10% concentration), H_2O_2 (20% concentration). Remaining sediment residue was found to be clay-rich and, therefore, further treatment was forced to a “fine-grain” poly-mineral approach. Material was subjected to fractionation isolating the 4–11 μm particle-size fraction. The quantity of the fine-grain fraction was then divided in sub-samples (aliquots) and mounted on stainless disks (1 cm in diameter). Luminescence measurements were carried out using a RISØ-TL/OSL-15 reader. Paleodose measurements were carried out running the “post-infrared OSL” (pIR-OSL) protocol by Banerjee et al. (2001) on multiple aliquots (~10 aliquots/sample), generating in this way a number of individual paleodoses per sample. Specifically, measurement of natural IRSL and OSL signals were succeeded by the measurement of IRSL and OSL responses to a series of regenerated laboratory irradiations, all normalized by the IRSL and OSL response to a constant laboratory dose respectively, known as the “test dose” (Murray and Wintle, 2000). Concentrations of U and Th (in ppm) and K (in % by weight) were converted to dose rate units by taking into account conversion factors published by Adamiec and Aitken (1998). The dose rate values were further corrected for moisture content, grain-size attenuation and cosmic-ray contribution.

3.4. Palaeontology

In total, 57 dried samples from core G-1 and 48 from core G-2 of approximately 50 g each, were picked for macro- and microfaunal analyses. When large mollusc shells were detected after careful macroscopic inspection of the cores, additional sediment samples were collected in order to determine molluscan assemblages. Consequently, 21 additional samples from core G-1 and 6 from core G-2 were also collected for macrofaunal analyses, and in this case the respective sediment samples exceeded 50 g. Subsequently, the specimens were washed through 0.5 and 0.063 mm mesh sieves using tap water. Macrofaunal specimens were mainly collected from the 0.5 sieve. When possible, no < 300 tests per sample (ostracods, foraminifera and small molluscs) were handpicked from the 0.063 mm mesh sieve sediment fraction. The collected specimens were sorted, determined, if possible, to species level, and counted. Taxonomic information was checked and updated using the World Register of Marine Species (WoRMS, 2015). The microfossil remains were grouped based on their ecological requirements and are presented as percentage diagrams. As far as the macro-fauna is concerned the relative abundance of each identified taxon was estimated.

In addition 32 sediment samples from core G-1 were selected for dinoflagellate analysis. The dinoflagellate preparation followed standard techniques including sediment freeze-drying, weighing, treatment

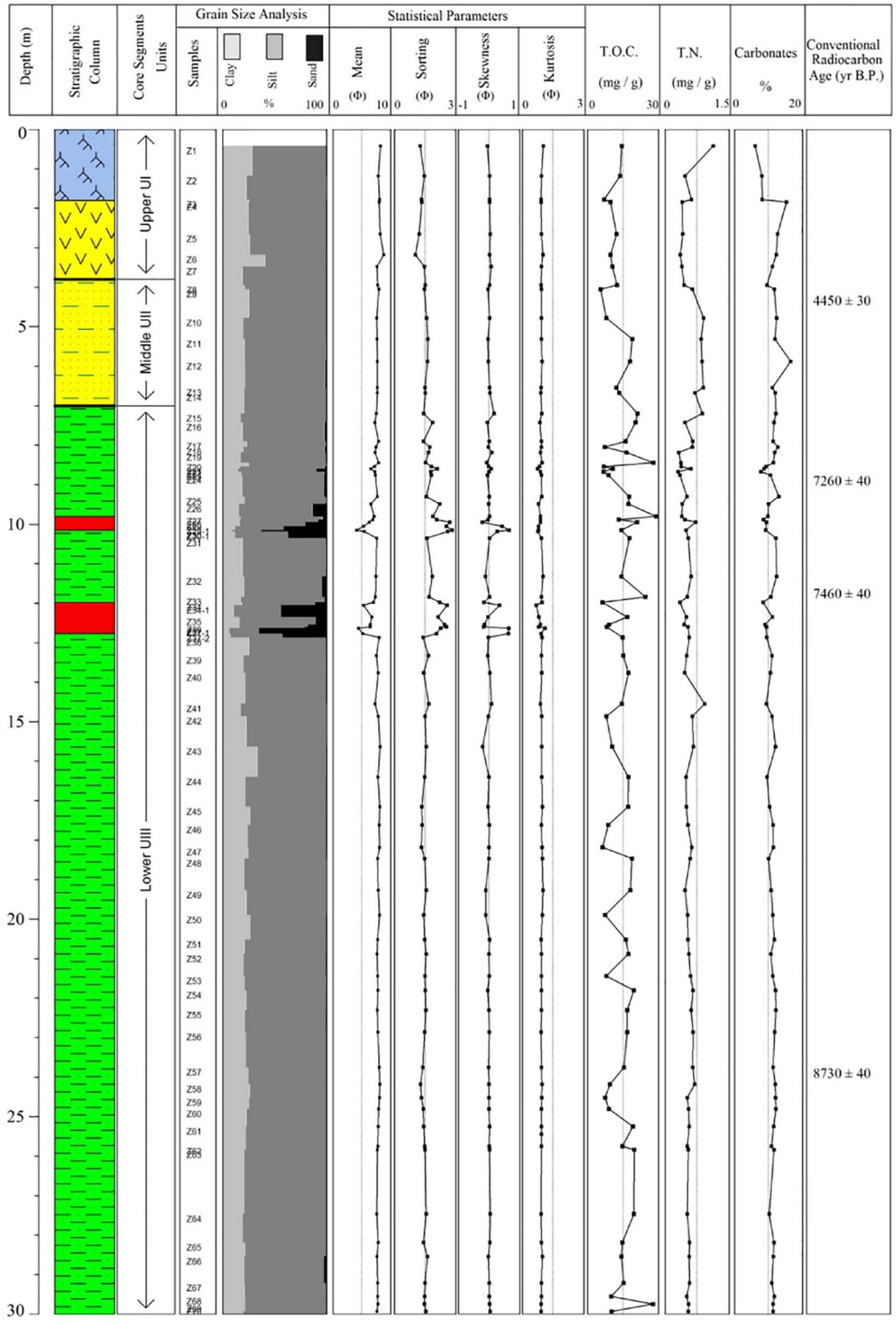

Fig. 3. Log profile of the core G-1 showing the lithological units, grain size distribution and statistical parameters, total organic carbon (TOC), total nitrogen (TN) and carbonate contents, and radiocarbon datings.

with HCl (> 30%) and HF (40%), sieving (10 μm), and mounting on glass slides. All samples were spiked with *Lycopodium* spores to facilitate the calculation of dinocyst accumulation rates and were analyzed using a Zeiss Axioskop light microscope at 400 × magnification.

4. Results

4.1. Lithostratigraphy

Based on the field description, the sedimentary structures, the

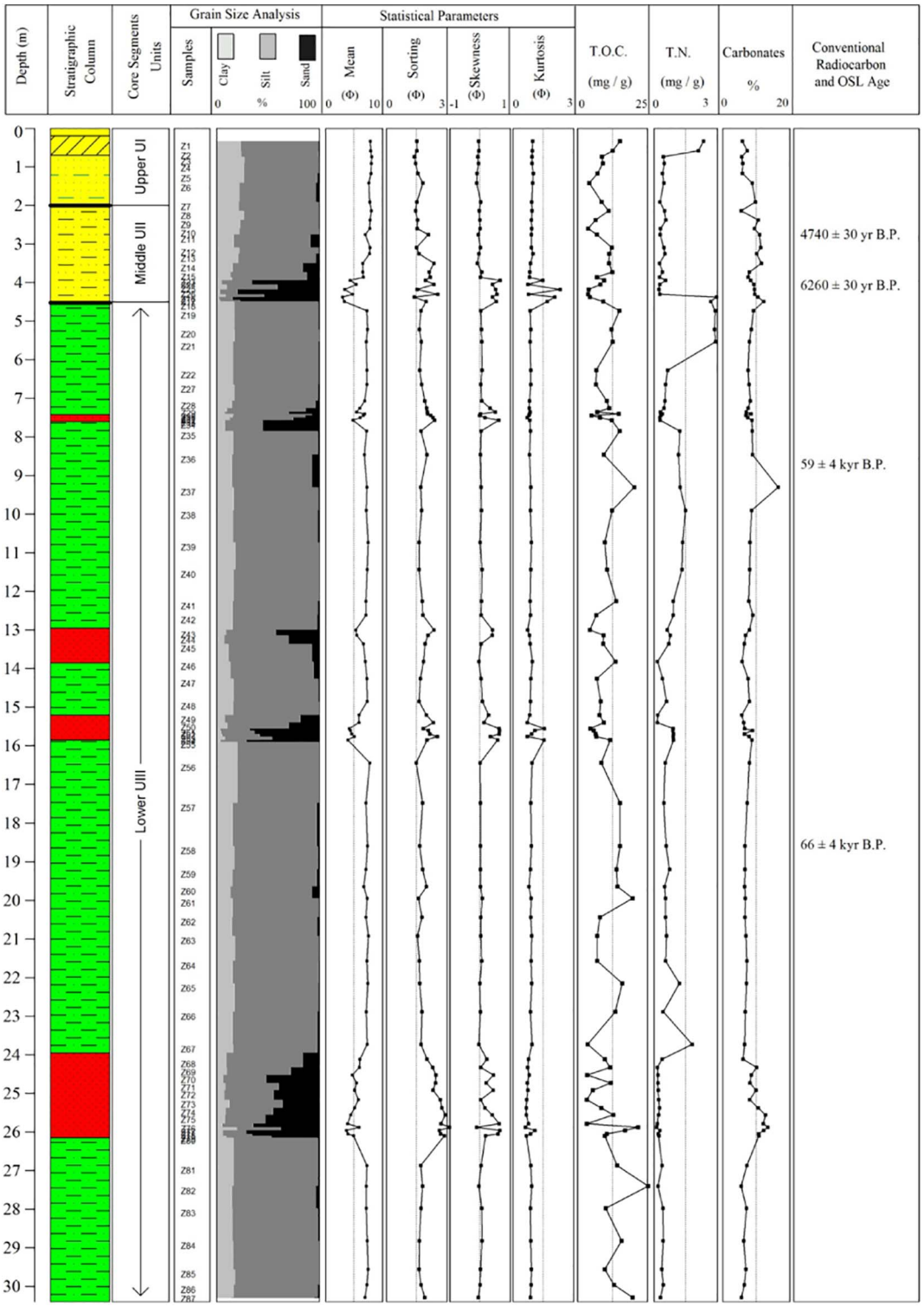

Fig. 4. Log profile of the core G-2, showing the lithological units, grain size distribution and statistical parameters, total organic carbon (TOC), total nitrogen (TN) and carbonate contents, and the radiocarbon and OSL datings.

colour and the grain size analyses, cores G-1 and G-2 were divided into three sedimentary units (Figs. 3 and 4). In core G-1, the upper unit UI is from 0.0–3.8 m, the middle UII from 3.8–7.0 m and the lower UIII from 7.0–30.0 m, while in core G-2 the upper unit UI is from 0.0–2.0 m, the middle UII from 2.0–4.5 m and the lower UIII from 4.5–30.3 m (Figs. 3 and 4). In the following, we describe the sedimentological characteristics of these units for each core individually.

4.1.1. Core G-1

Upper Unit (Unit I, 0.0–3.8 m) consists of poorly sorted, olive grey to greyish brown, very fine silt to mud, while sand is almost absent. Values of sorting range between 1.0 and 1.5 Φ, with mean values ranging between 7.6 and 8.8 Φ. Skewness values indicate a symmetrical distribution and kurtosis values show a mesokurtic distribution. Ostracods and gastropods are abundant between 1.8 and 3.8 m core depth and several bivalves are present. The carbonate content ranges

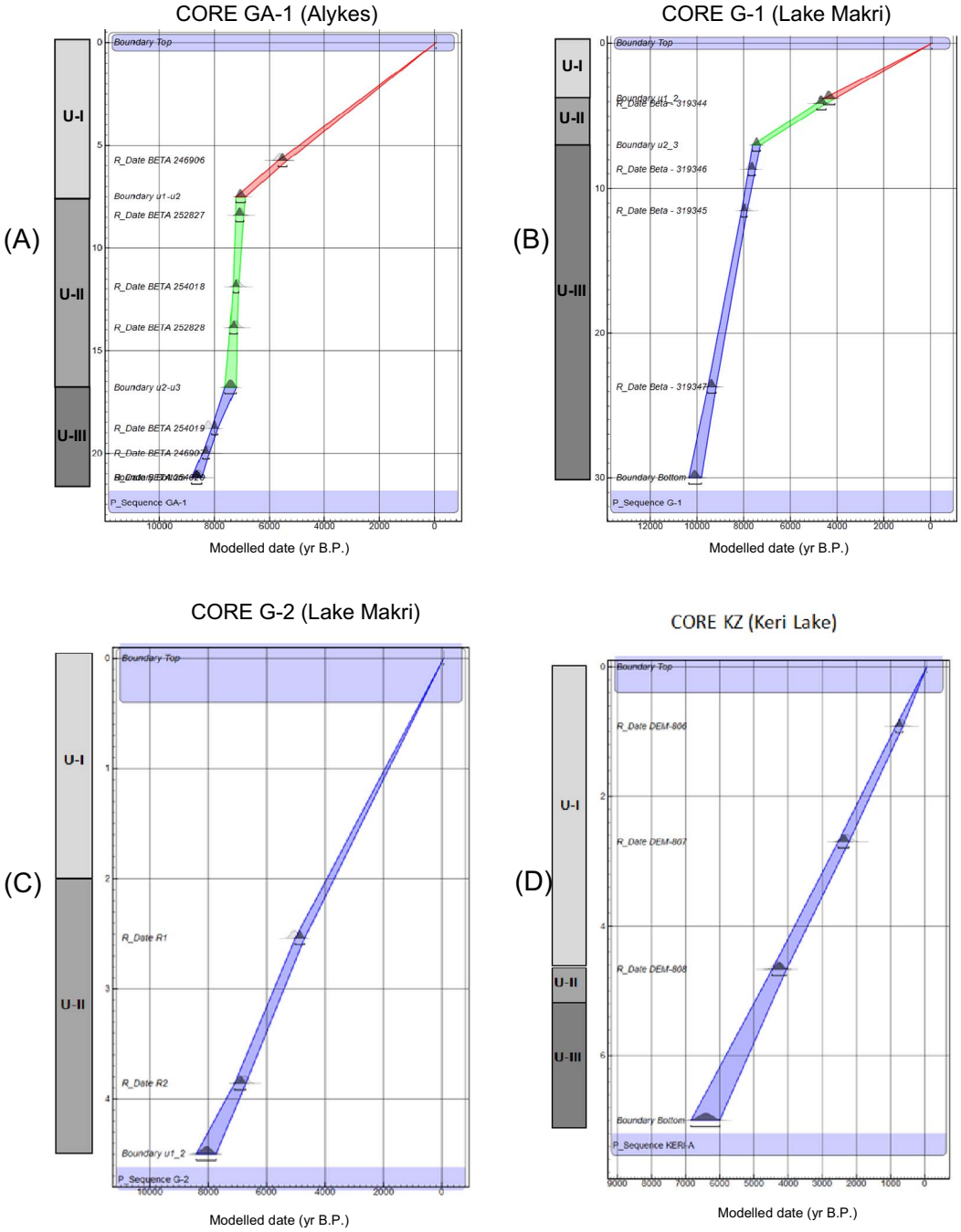

Fig. 5. Lithological units and age depth models for the cores (A) GA-1 (re-evaluated data from Avramidis et al., 2013), (B) G-1 this study, (C) G-2 this study and (D) KZ (re-evaluated data from Papazisimou et al., 2000; Avramidis et al., 2017).

between 6.1 and 15.2%, TOC between 7.0 and 14.3 mg/g, and TN between 0.3 and 1.1 mg/g, while a break of the above parameters at 1.8 m depth is observed corresponding to the subunit between 0.0 and 1.8 m which has been influenced by anthropogenic activities (cultivation, etc.) (Fig. 3).

Middle Unit (Uniti II, 3.8–7.0 m) consists of poorly sorted, olive grey to greenish grey, very fine silt to silt; sand is rare, similar to Unit I. Values of sorting range between 1.5 and 1.6 Φ, with mean values ranging between 7.6 and 8.0 Φ. Skewness values indicates a symmetrical distribution and kurtosis values show a mesokurtic distribution with an exception of one sample that is platykurtic. A relative increase in the presence of shells and shell fragments is recorded, with ostracods and gastropods being abundant and several bivalves present. The carbonate content ranges between 9.5 and 16.5%, TOC between 5.4 and 18.9 mg/g, and TN between 0.4 and 0.9 mg/g (Fig. 3).

Lower Unit (Unit III, 7.0–30.0 m) consists of poorly to very poorly sorted, light greenish grey to dark olive grey, fine silt to sandy mud, and in some intervals of very fine sand. Mean values for the unit range between 4.0 and 8.2 Φ. Silt and mud layers are characterized by symmetrical and mesokurtic distributions and are intercalated with two main horizons of poorly sorted, very fine sand (9.8–10.1 m and 12.0–12.8 m). The sand intercalations are very poorly sorted and no uniform distribution characteristics were observed. Contacts between silt and sand layers are characterized as slightly erosional. Major characteristic of this unit is the presence of scaphopods in the lower part between 28.0 and 29.5 m depth. The carbonate content ranges between 7.8 and 13.0%, TOC between 6.2 and 29.0 mg/g, and TN between 0.3 and 0.9 mg/g (Fig.3).

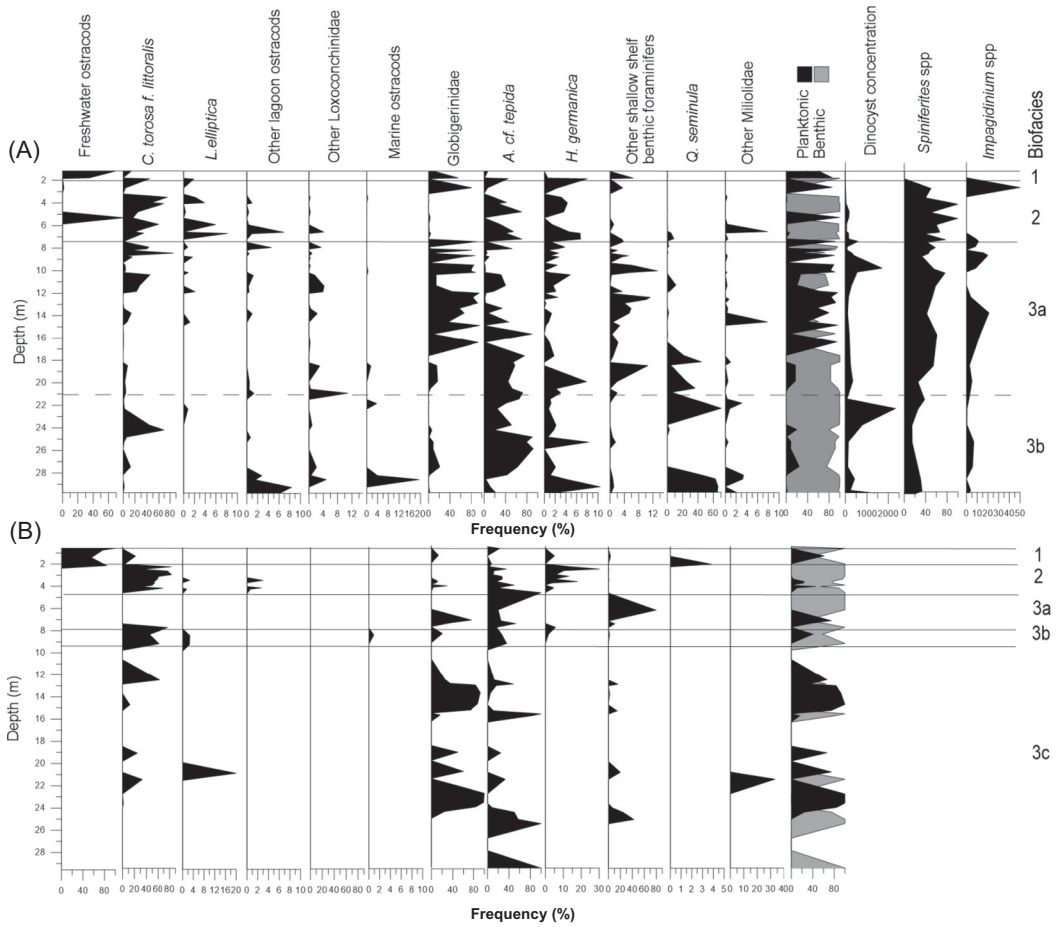

Fig. 6. Percentage diagrams of selected microfossil taxa and groups of taxa, planktonic vs. benthic foraminifera abundances and total dinoflagellate cyst concentrations recorded in cores G-1 (A) and G-2 (B) plotted against depth. Microfossil groups are based on the ecological requirements of individual taxa.

4.1.2. Core G-2

Upper Unit (Unit I, 0.0–2.0 m) consists of poorly sorted, greyish to dark olive, very fine to fine silt with the abundance of sand being < 5%. Values of sorting range between 1.4 and 1.8 Φ, with mean values ranging between 7.6 and 8.1 Φ. Skewness indicate a symmetrical distribution and values of kurtosis show a mesokurtic distribution. No macrofossils are present. The carbonate content ranges between 5.5 and 9.5%, TOC between 4.2 and 15.1 mg/g, and TN between 0.3 and 2.3 mg/g (Fig. 4).

Middle Unit (Unit II, 2.0–4.5 m) consists of poorly to very poorly sorted, greyish to dark olive, very fine to fine silt with increasing abundance of sand with depth (> 50%). Values of sorting range between 1.4 and 2.3 Φ, with mean values ranging between 4.3 and 8.0 Φ. Skewness indicate a symmetrical to very fine skewed distribution and values of kurtosis show a mesokurtic distribution. In this unit abundant ostracods and gastropods and several bivalves and shell fragments are present. The carbonate content ranges between 5.4 and 11.3%, TOC between 3.7 and 12.4 mg/g, and TN between 0.2 and 0.6 mg/g (Fig. 4).

Lower Unit (Unit III, 4.5–30.3 m) consists of poorly to very poorly sorted, grey to olive grey and greenish grey, muddy silt with the presence of four intercalated sand layers (at 7.42–7.60 m, 12.95–13.85 m, 15.2–15.85 m, and 23.95–26.15 m). Values of sorting range between 1.3 and 3.1 Φ, with mean values ranging between 2.2 and 7.7 Φ. Skewness indicates a symmetrical distribution in the mud layers, while a very finely skewed to coarsely skewed distribution is observed in the sand layers. Kurtosis indicates different patterns of distribution. No macrofossils are present. The carbonate content ranges between 5.4 and 16.2%, TOC between 3.2 and 25.9 mg/g, and TN between 0.1 and 3.0 mg/g (Fig. 4).

4.2. Chronology – age-depth model

The chronostratigraphy of cores G-1, G-2, GA-1 and KZ were determined by sixteen ^{14}C and two OSL dates (Tables 1 and 2) using Oxcal 4.1 software; age depth curves are presented in Fig. 5. All ^{14}C and OSL dates are in sequence, and no anomalously young dates were observed. Based on the calculated age-depth model, the chronological boundaries for each lithostratigraphic unit were estimated and different rates of sedimentation were calculated (Fig. 5). Various sedimentation rates have been reconstructed with the highest ones observed for the interval before 7000 yr B.P. in the northern core GA-1 (40.0 mm/yr) and southern core G-1 (9.2 mm/yr) (Fig. 5). Lower sedimentation rates are recorded from 6000 yr B.P. to present for both northern (1.0 mm/yr) and southern (1.1 mm/yr) cores. High sedimentation rates observed in Zakynthos Island correspond well to the most widespread Holocene warm and humid phases and to periods of fast sea level rise (Vött, 2007). The shift towards lower sedimentation rates after ~7000 yr B.P. onwards could be associated with a slowdown of the sea level rise, which for western Greece it was suggested have started at around 6000 yr B.P. (Vött, 2007; Brückner et al., 2010). In core G-2, the OSL dates of 59–64 kyr B.P. in unit UIII suggest that there is a hiatus due to an unconformity between units UII and UIII (Fig. 4; Tables 1 and 2).

4.3. Palaeontology

4.3.1. Core G-1

The biostratigraphical description of G-1 core is based on the discrimination of three major biostratigraphical units as follows (Fig. 6A): Biofacies 1 - B1 (depth 0.0–1.8 m), Biofacies 2 - B2 (depth 1.8–7.0 m),

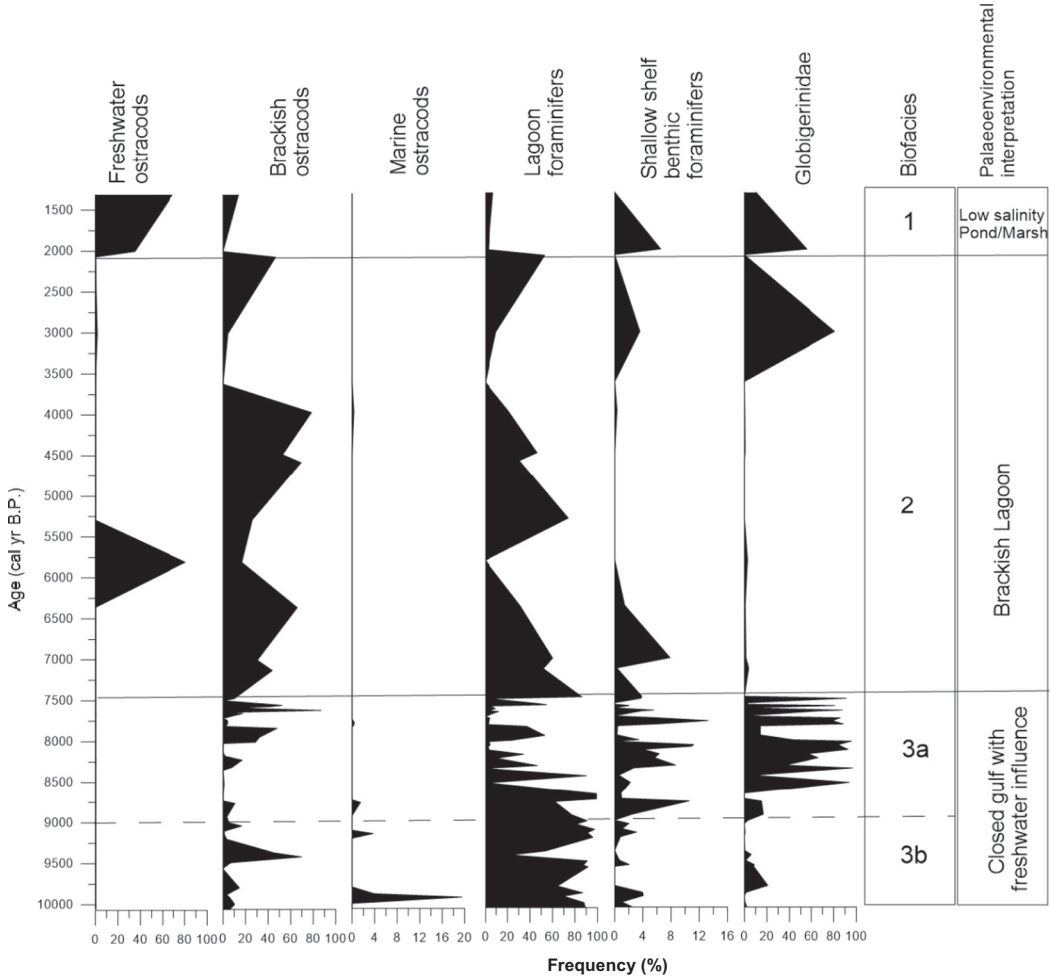

Fig. 7. Percentage diagrams of selected microfossil groups of taxa recorded in core G-1 plotted against age. Major biofacies and their palaeoenvironmental interpretations are also presented.

Biofacies 3 - B3 (depth 7.0–30.0 m). The determination of these units was based on the macro- and microfossil taxa assemblages. All units contain varied proportions of bivalves, gastropods, ostracodes, foraminifera tests and cysts of dinoflagellates (dinocysts), whereas in the upper three meters of the core charophyte gyrogonites are present and dinocysts disappear. In the lower two meters some rare scaphopods are found and in the middle and lower part of the core a few sea urchin spines.

In Biofacies 1 (B1: 0.0–1.8 m), the dominant taxa are the ostracod *Herpetocypris reptans* and the small fresh water gastropod *Valvata piscinalis* (Grigorovich et al., 2005) (Fig. 6A). These two and in addition the presence of *Limnocytherina sanctipatricii*, *Valvata cristata* and charophyte gyrogonites and the total absence of dinocysts (Fig. 5A) indicate a limnic assemblage (Meisch, 2000; Guiry and Guiry, 2008; Krzymińska and Namiotko, 2012), most likely a pond or marsh with salinity 0.5–6‰ as has been suggested for the stenohaline *H. reptans* (Hiller, 1972). However, the low presence of *Cyprideis torosa f. littoralis*, *Ammonia tepida*, *Quinqueloculina seminula*, *Cerastoderma glaucum*, *Abra segmentum*, *Hydrobia acuta*, *Cyclope neritea* and *Potamides conicus* and also the presence of a significant number of Globigerinidae and some shallow shelf benthic foraminifera (Fig. 6A) suggest a close proximity to brackish and marine environments (Kilenyi and Whittaker, 1974; Heip, 1976; Debenay et al., 2000; Torres et al., 2003).

In Biofacies 2 (B2: 1.8–7.2 m), the dominant taxa are *C. torosa f. littoralis*, *Loxoconcha elliptica*, *A. tepida*, *Haynesina germanica*, *C. glaucum*, *A. segmentum*, *H. acuta*, *C. neritea* and *P. conicus*, which together with other lagoon ostracods and molluscs that are found in lower numbers, are indicative of a brackish lagoon environment (Taraschewski and Paperna, 1981; Bignot, 1985; Meric et al., 2001; Torres et al., 2003). Significantly low numbers of dinocysts are found in this biofacies (Fig. 6A). *Spiniferites* spp. are dominating, with relative abundances up to 80%, which points to a brackish environment possibly with freshwater incursions (Verleye et al., 2009; Shumilovskikh et al., 2013).

The Biofacies 3 (B3: 7.2–3 m), can be further divided in two subbiofacies with distinct faunal assemblages: sub-biofacies 3a (SB 3a: depth 7.2–20.9 m) and sub-biofacies 3b (SB 3b: depth 20.9–30.0 m) (Fig. 6A).

In the sub-biofacies 3a (SB 3a: depth 7.2–20.9 m), *A. tepida* dominates and *H. germanica* is also present with low abundances. *Q. seminula* is present with high abundances (22–45%) in the lower part, while in the upper part other shallow shelf benthic foraminifera are present in small numbers. *H. acuta*, *C. glaucum* and *A. segmentum* are also present in low numbers. The distinct presence of *Corbula gibba* in the upper part of this sub-biofacies suggests possible prevalence of dysoxic/hypoxic conditions and high contents of organic matter. This species lives in sandy muds and is quite tolerant of salinity changes and oxygen depletion, even at the levels of anoxia (Holmes and Miller, 2006). *A. tepida and H. germanica* can also survive under hypoxic conditions (Gupta, 2003). The total concentration of dinocysts shows a small but considerable increase within sub-biofacies 3a. *Spiniferites* spp. is the dominant dinocyst, showing that brackish conditions are prevailing. The composition of the faunal assemblage suggests a shallow marine environment such as a closed gulf. This is supported by the total

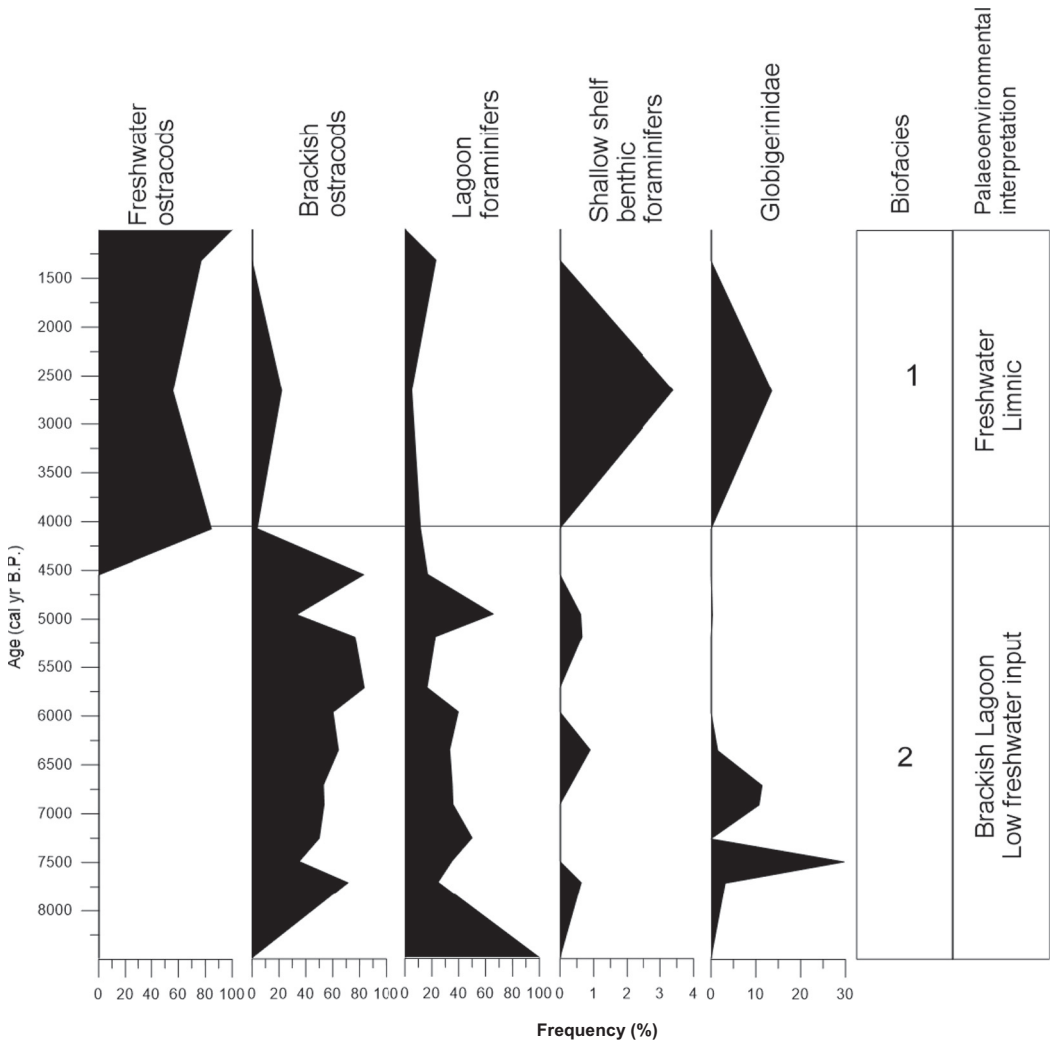

Fig. 8. Percentage diagrams of selected microfossil groups of taxa recorded in core G-2 plotted against age. Major biofacies and their palaeoenvironmental interpretations are also presented.

absence of the typical brackish taxon *C. torosa f. littoralis* (Frenzel and Boomer, 2005). This sub-biofacies between 7.4 and 16.4 m is also characterized by the exceptionally high numbers of Globigerinidae and the relatively higher abundances of shallow shelf benthic foraminifera, such as *Bolivina* spp., *Bulimina* spp., *Cibicides* spp. and *Uvigerina* spp., compared to the other horizons. This reveals increased influx of marine originated deposits into a lagoonal environment. On the contrary, typical lagoon taxa are underrepresented (e.g., *A. tepida*) or even become absent (e.g., *C. torosa f. littoralis*). Furthermore, the sand component in the sediments becomes dominant.

In the sub-biofacies 3b (SB 3b: depth 20.9–30.0 m), *A. tepida and H. germanica* are the dominant species in this unit (Fig. 6A). The concentration of dinocysts increases especially in the upper part (21.44–25.25 m), while the relative abundance of *Spiniferites* spp. shows a decrease (maximum percentages 40%). This could be the result of increased salinity due to marine influence, as suggested by the increase of fully marine dinoflagellate taxa such as *Impagidinium* spp. (Fig. 6; e.g., Kotthoff et al., 2011). The assemblage can be characterized as a closed gulf with brackish waters. Additionally, *C. gibba* dominates the macrofaunal realm in the lower part of this subunit, suggesting possible dysoxic/hypoxic conditions and high contents of organic matter, as it is quite tolerant of changes in salinity and oxygen deprivation (Holmes and Miller, 2006). A small venerid bivalve (*Chamelea* cf. *striatula*) and scaphopods (*Atlantis* cf. *inaequicostata*) are also present. Dysoxia/hypoxia prevailed as pointed out by the dominance of *C. gibba* and *Q. seminula*. *C. gibba* can tolerate hypoxia even in brackish conditions and becomes the dominant taxon under hypoxia (Holmes and Miller, 2006). *A. tepida*, *H. germanica* and *Q. seminula* are also dominant in the lower part of this subunit and indicate prevalence under hypoxic/dysoxic conditions (Gupta, 2003). The occasional presence of *C. torosa f. littoralis* at the upper part of this sub-biofacies indicates transient periods of lower salinity levels.

4.3.2. Core G-2

The biostratigraphical description of G-2 core is based on the discrimination of three major biofacies as follows (Fig. 6B): Biofacies 1 - B1 (depth 0.0–2.2 m), Biofacies 2 - B2 (depth 2.2–4.5 m), and Biofacies 3 - B3 (depth 4.5–30.0 m). The determination of these units was based on the macro- and microfossil assemblages. All units contain varied proportions of bivalves, gastropods, ostracodes and foraminifera tests, whereas only Biofacies 1 contains charophyte gyrogonites.

In Biofacies 1 (B1: depth 0.0–2.2 m), freshwater ostracods and gastropods such as *H. reptans*, *I. bradyi*, and *V. piscinalis* (Hiller, 1972; Grigorovich et al., 2005) are the dominant taxa in this unit suggesting a limnic environment. The fresh water character of the sediments is also verified by the high abundances of charophyte gyrogonites (Guiry and Guiry, 2008).

In Biofacies 2 (B2: 2.2–4.5 m), the dominant taxa in this unit are *C. torosa f. littoralis*, *A. tepida*, *H. germanica*, *C. glaucum*, A. *segmentum* and *H. acuta* accompanied by the sporadic presence of other lagoonal

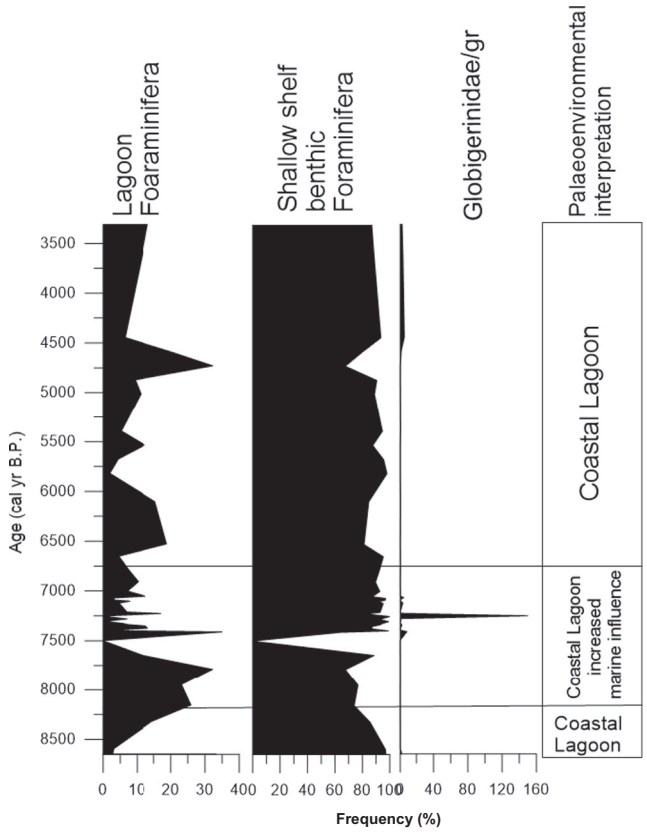

Fig. 9. Percentage diagrams of selected microfossil groups of taxa from core GA (Alykes Lagoon; Avramidis et al., 2013) and palaeoenvironmental interpretation as a function of age.

ostracods (e.g., *Leptocythere* cf. *lacertosa*, *L.* cf. *elliptica*) (Bignot, 1985; Frenzel et al., 2010) and *P. conicus*. This assemblage indicates a lagoonal environment with salinity > 10‰. The presence of a noticeable number of Globigerinidae tests between 3.73 and 4.50 m suggests transport of marine sediments perhaps related to storm events. A few sparse fresh water elements (e.g., *V. piscinalis*) indicate some temporary fresh water influence.

In Biofacies 3 (B3: 4.5–30.0 m) the number of taxa and the number of collected foraminifera tests is reduced drastically to < 5 specimens; in addition, ostracod valves disappear completely. This indicates prevalence of unfavorable conditions for their survival, possibly anoxia. Nevertheless, at 7.5 m core depth *A. tepida* is present accompanied by a few shallow shelf benthic foraminifera and a proportionally increased abundance of Globigerinidae. These taxa represent a shallow marine environment, such as a closed gulf, which is affected by high energy events like storms or tsunamis. This biofacies can be separated further into three sub-biofacies, i.e., SB1 (depth 4.50–7.84 m), SB2 (depth 7.84–9.30 m) and SB3 (depth 9.3–30.0 m). According to OSL dating from this part of the core the age of the sediments lies within the Late Pleistocene (older than 50 kyr B.P.; Table 2), pointing to the existence of a hiatus due to an unconformity located below biofacies B2. As such, this precludes further analysis of this biofacies.

5. Discussion

5.1. Palaeoenvironmental evolution

The sedimentological and paleontological results from the new cores G-1 and G-2 and the already published cores of GA-1 (Avramidis et al., 2013) and KZ (Papazisimou et al., 2000) indicate that the palaeoenvironments of the coastal areas of Zakynthos Island progressively changed from marine (enclosed shallow gulf) to lagoon and coastal lake depositional environments (Figs. 7–10). The palaeonvironmental interpretations reveal that during the early Holocene and prior to 7500 yr B.P. Zakynthos was separated into two smaller islands (Fig. 11A). Vasilikos peninsula was detached from the rest of the island and after that period gradually lagoon barriers started to develop. This resulted in the accumulation of lagoonal and limnic deposits (Fig. 11B,C) and ultimately Vasilikos peninsula merged with the rest of Zakynthos Island as it stands today. The onset of the sand barriers development occurred at around 7000 yr B.P. as recorded both in the north (core GA-1), and around 7500 yr B.P. in the south (cores G-1 and G-2). According to Kraft et al. (2005), sand barriers started to developed around the same time (8000 yr B.P.) in the shallow inner shelf of Elis, an area which is located at the western coast of the Peloponnese ~40 km east of Zakynthos Island (Fig. 1B). These palaeonvironmental changes and coastal processes in western Greece were controlled mainly by the eustatic sea level changes (Vött, 2007), changes in the sources of sediment supply and the impact of tectonic events (Vött and Kelletat, 2015).

The evolutionary model of Zakynthos coastal evolution is presented in Fig. 11 and is based on four different chronological stages according to sedimentary units and biofacies interpretations. Between 10,000 and 7500 yr B.P., the area around core G1 can be considered to be a restricted, shallow gulf with fresh water influence. This is suggested by alternations of brackish ostracods and lagoon foraminifera with shallow shelf benthic foraminifera (Fig. 7). During the period 9000 to 7500 yr B.P. (Biofacies 3a) increased marine influence is witnessed by the observed high percentages of Globigerinidae and fully marine dinocysts (e.g., *Impagidinium* spp.). Since 7500 yr B.P. and until 2100 yr B.P. (Biofacies 2) a brackish lagoon was established around the area of core G1, as indicated by the high percentages of brackish ostracods and lagoonal foraminifera (Fig. 7). Similarly, the area around core G2 can be also characterized as a brackish lagoon with a low freshwater input from around 7500 to 4100 yr B.P. (Biofacies 2), as revealed by the high percentages of brackish ostracods and the absence of freshwater ones (Fig. 8). Between 7500 and 6500 yr B.P., a high percentages of Globigerinidae are also noticeable and indicate an increased marine influence, possibly correlating to the Biofacies 3a (until 7500 yr B.P.) of core G1. Around 4000 yr B.P. a barrier was established in the area of core G2 and the brackish lagoon converted into a freshwater/lacustrine environment, as suggested by the increase of freshwater ostracods at the expense of the brackish/marine ones (Biofacies 1). The transitional from a brackish lagoon to a low salinity pond/marsh palaeoenvironment at the area around core G1 only occurred at around 2100 yr B.P. (Biofacies 1) (Figs. 8 and 11).

As discussed above, between 7500 and 6500 yr B.P. the core sites were under a strong marine influence, with the area around core G1 being more influenced than that around G2. This is in agreement with the documentation of a marine influence event in a brackish coastal lagoon that has been reported in core GA (Avramidis et al., 2013) between 8000 and 6400 yr B.P. (Fig. 9). This event is documented by the highly variable percentages of lagoon foraminifera during this time interval and the extremely increased number of Globigerinidae at around 7250 yr B.P. (Fig. 9).

Between 7500/6500 yr B.P. and 4000 yr B.P. the brackish lagoon shows no marine influence (cores G1, G2). This is in agreement with the evidence for a brackish lagoon with low marine influence in core GA (Avramidis et al., 2013) as suggested by the higher percentages of lagoon foraminifera and the very low amounts of Globigerinidae (Fig. 9). In contrast, the very high percentages of Globigerinidae and the relatively high percentages of shallow shelf foraminifera at Keri show evidence for significant marine influence between 6000 yr B.P. and 4000 yr B.P. (Fig. 10). Subsequently, the establishment of a small closed gulf with fresh water influence at Keri between 4000 and 3500 yr B.P. is evidenced by the concurrent presence of shallow shelf foraminifera-Globigerinidae and freshwater/low salinity ostracods - marine brackish ostracods (Fig. 10).

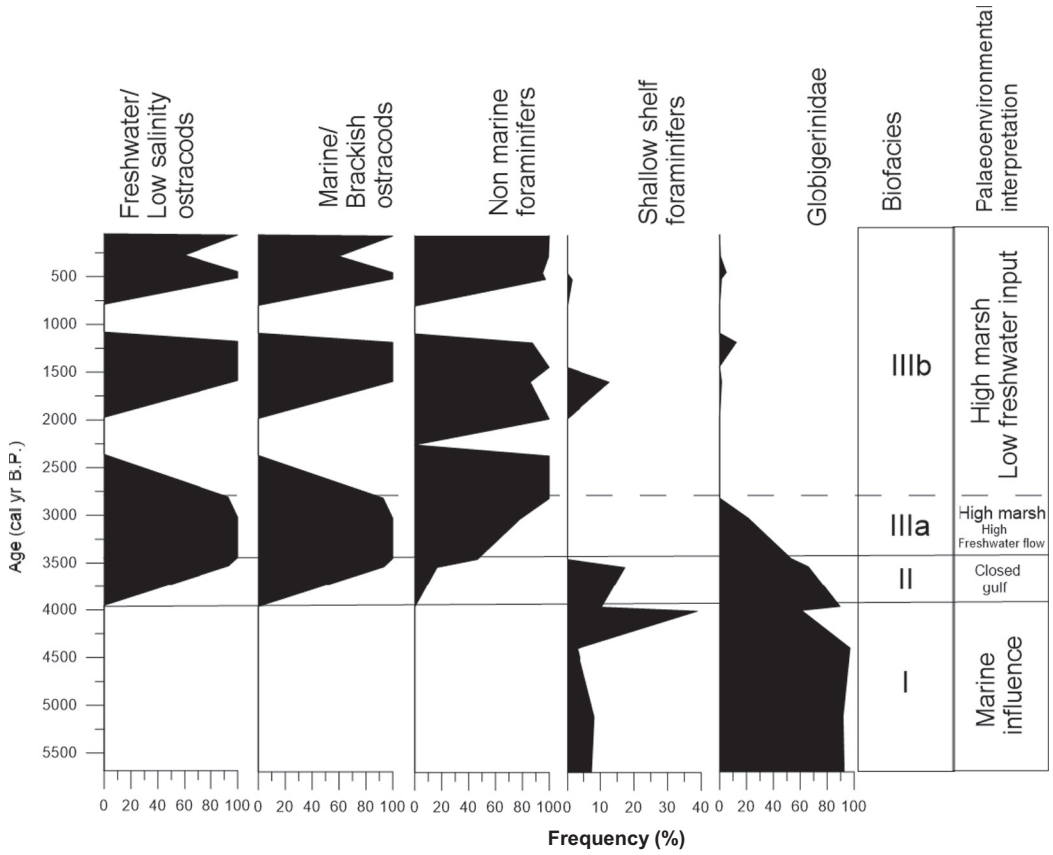

Fig. 10. Percentage diagrams of selected microfossil groups of taxa from core KZ (Keri Lake; Papazisimou et al., 2000, Avramidis et al., 2017), biofacies and palaeoenvironmental interpretation as a function of age.

Around 4000/3500 and 2000 yr B.P. a barrier was built and a freshwater limnic environment was established at the sites of core G2 and G1, respectively, forming Lake Makri (Fig. 11C). The same process was also started at Keri, while the brackish lagoon was still prevailing at G1. Eventually, after 2000 until 130 yr B.P., G-1 and G-2 were both converted to freshwater-low salinity environments, while a low salinity/pond marsh was developed at Keri (core KZ), as suggested by the high percentages of freshwater ostracods. After 130 yr B.P. (around 1820 CE) Lake Makri was drained for agricultural purposes and today this area is covered by the airport of Zakynthos Island.

5.2. *Examples from eastern Mediteranean - implication for archaeological research*

The considerable deceleration of the transgression around 7000 years ago led to the formation of deltas (Stanley and Warne, 1994), delta progradation and shoreline dislocation (Morhange and Marriner, 2010). As the result of the deltas's progradation, marine embayments, estuarines and gulfs were silted up. In a smaller scale this phenomenon is observed in our study in Zakynthos Island where during the Holocene in the central part of the island the depositional environments changed gradually from marine, to lagoon and finally to limnic, merging the Vasilikos peninsula (palaeoisland) with the rest of the island of Zakynthos (Fig. 11A–D). This sedimentological process caused the attachment or 'landlocking' of the Vasilikos peninsula around 7500 yr B.P. (Fig. 11). There are several examples in the Mediterranean region describing similar sedimentological processes of 'landlocking islands' with deltaic progradation or associated with tombolos. Most of them are located in coasts of Turkey, in the areas of Miletus, Ephesus and Troy (Kraft et al., 1977, 1980; Brückner, 2005; Brückner et al., 2002, 2005; Kraft et al., 2003, 2007). Examples in Greece include Oiniades and Echinades palaeoislands in the Acheloos River delta (Vött et al., 2007) and in Egypt the Alexandria Tyre tombolo (Anthony et al., 2014).

The Holocene coastal geomorphology and archaeological landscape of Zakynthos as well as the Ionian Islands during the last decades concentrated the interest of geologists and archaeologists (Underhill, 2009; Tendürüs et al., 2010; Gouma et al., 2011; Van Wijngaarden et al., 2013). This interest arose from the fact that the Ithaca Island, the Homeric island of the epic Greek king Odysseus, is located very close to Zakynthos Island (Fig. 1B). Moreover, several different ideas and criticisms concerning the geography described in the Odyssey, have been written, and a debate has emerged about the location of Homeric Ithaka and Odysseus' palace (Underhill, 2009).

The fact that during most of prehistory Vasilikos was separated from the rest of the Zakynthos is of importance for the interpretation of the results of the archaeological research which has been carried out on the island. The peninsula of Vasilikos has yielded material remains from all periods since early prehistory (Van Wijngaarden et al., 2013). Of particular importance is the fact that the abundant lithic artefacts found at Vasilikos have been made from pebble flint, which was probably collected from secondary sources such as terraces and beaches. This is in contrast to the lithic artefacts elsewhere on Zakynthos, which are made from flint nodules that occur in the western hills of the island. The abundance of flint pebble tools at Vasilikos, with different degrees of patina, suggest that they may have been produced through the Palaeolithic period and even during later prehistory (cf. Darlas, 1999). The different raw materials used at Vasilikos, corresponds to the physical separation between the two parts of the island in early prehistory. A similar distinction in material culture between the two parts of the island can, as yet, not be distinguished for the artefacts dating to later periods.

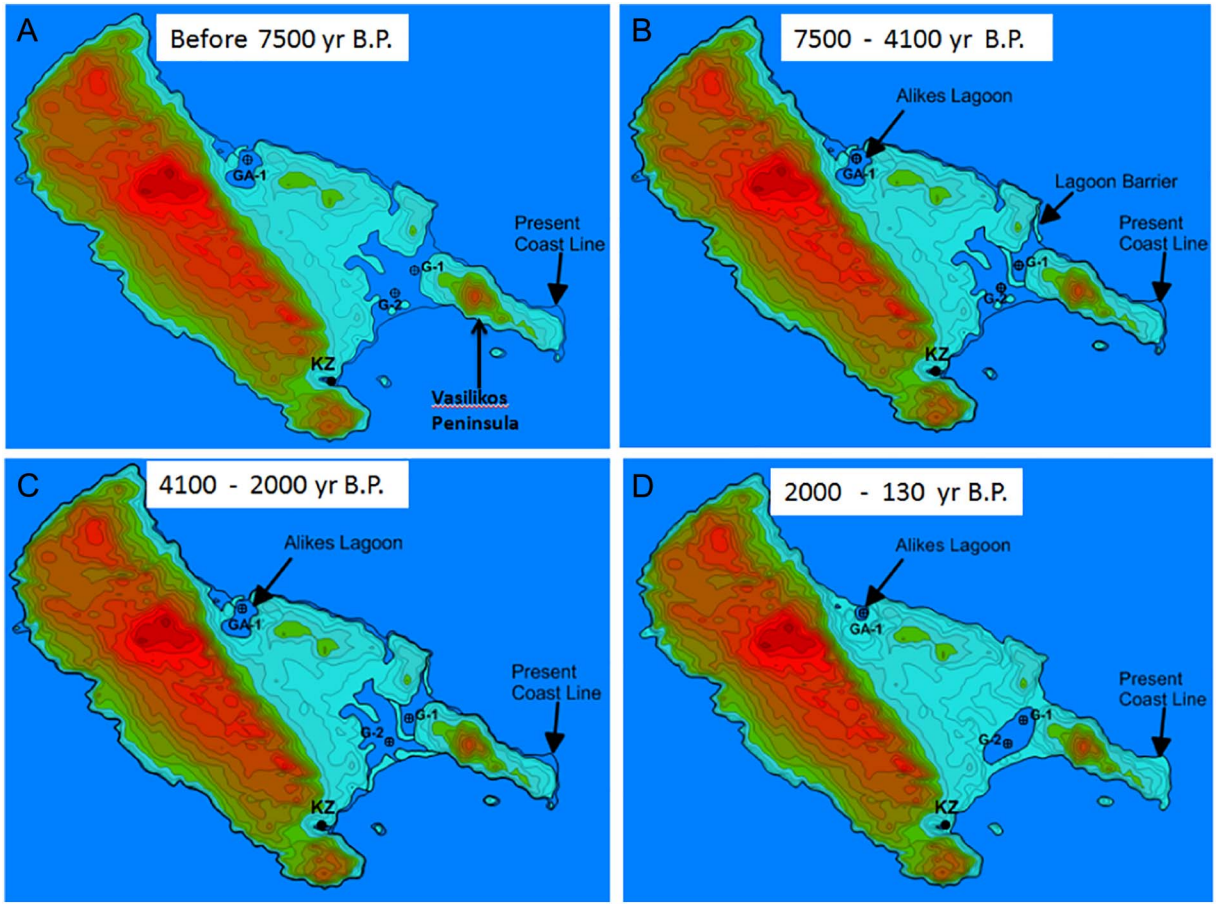

Fig. 11. Reconstruction of Holocene coastal environmental changes of Zakynthos Island, which is based on the 5 m contour lines, produced using SRTM (Shuttle Radar Topography Mission, NASA).

6. Conclusions

The study and comparison of the four cores from Zakynthos Island indicate that its coastal depositional environments have been subjected to several geomorphological changes during the Holocene. The combination of sedimentological and palaeontological data within a robust chronostratigraphic scheme allowed the reconstruction of landscape and palaeonvironmental evolution of the island for the past ~10,000 years. Four evolutionary stages were recognized: (a) before 7500 yr B.P., (b) between 7500 and 4100 yr B.P., (c) between 4100 and 2000 yr B.P., and (d) from 2000 yr B.P. to present. During these individual chronological stages fully marine, lagoonal with marine influence, brackish and limnic depositional palaeonvironments were recognized, respectively. The fully marine and brackish lagoon conditions prevailed on the southwestern part of the island until 2000 yr B.P. Our data indicate that a lagoon was stretching at least from the Laganas Bay to the Zakynthos town until ~2000 yr B.P., hence, separating Vasilikos peninsula from the rest of the island. Our study indicates that during most the prehistory the Vasilikos peninsula was detached from the rest of Zakynthos Island and was acted as a separate 'palaeoisland'. The insight in the diachronic development of the landscape of Zakynthos shed a light and helps us to understand better the patterns of mobility and communication of the prehistoric humans in the Ionian Sea area contributing in the interpretation of the landscape evolution of the Ionian islands.

Acknowledgments

We would like to thank Dr. D.J.W. Piper (Bedford Institute of Oceanography, Geological Survey of Canada) for discussions and comments on an earlier version of the manuscript that greatly improved it. The fieldwork for this research has been made possible by a generous grant from the Institute of Aegean Prehistory (INSTAP) in New York. The research is conducted in the framework of the "Zakynthos Archaeology Project 2006–2015" at the University of Amsterdam, which is financed by the Dutch Organization for Scientific research (NWO) (file no. 380-60-003), the University of Amsterdam, INSTAP (INSTAP Grant 2011) (New York, USA) and the Utopa Foundation (project no. 2006248) (Leiden, the Netherlands).

References

Aberg, A., Lewis, C., 2000. The rising tide. In: Archaeology and Coastal Landscapes. Oxbow, Oxford.
Accordi, G., Carbone, F., Di Carlo, M., Pignatt, J., 2014. Microfacies analysis of deep-water breccia clasts: a tool for interpreting shallow- vs. deep-ramp Paleogene sedimentation in Cephalonia and Zakynthos (Ionian Islands, Greece). Facies 60, 445–465.
Adamiec, G., Aitken, M.J., 1998. Dose-rate conversion factors: update. Ancient TL 16 (2), 37–50.
Anthony, E.J., Marriner, N., Morhange, C., 2014. Human influence and the changing geomorphology of Mediterranean deltas and coasts over the last 6000 years: from progradation to destruction phase? Earth Sci. Rev. 139, 336–361.
Apostolopoulos, G., Pavlopoulos, K., Goiran, J.-P., Fouache, E., 2014. Was the Piraeus peninsula (Greece) a rocky island? Detection of pre-Holocene rocky relief with borehole data and resistivity tomography analysis. J. Archaeol. Sci. 42 (1), 412–421.
Avramidis, P., Geraga, M., Lazarova, M., Kontopoulos, N., 2013. Holocene record of environmental changes and palaeoclimatic implications in Alykes Lagoon, Zakynthos Island, western Greece, Mediterranean Sea. Quat. Int. 293, 184–195.
Avramidis, P., Iliopoulos, G., Panagiotaras, D., Papoulis, D., Lambropoulou, P., Kontopoulos, N., Siavalas, G., Christanis, K., 2014. Tracking mid- to late Holocene depositional environments by applying sedimentological, palaeontological and geochemical proxies, Amvrakikos coastal lagoon sediments, Western Greece, Mediterranean Sea. Quat. Int. 332, 19–36.
Avramidis, P., Kalaitzidis, S., Iliopoulos, G., Papadopoulou, P., Nikolaou, K., Papazisimou, S., Christanis, K., van Wijngaarden, G.J., 2017. The so called 'Herodotus Springs' at

'Keri Lake' in Zakynthos Island western Greece: a palaeoenvironmental and palaeoecological approach. Quat. Int. 439, 37–51.
Banerjee, D., Murray, A.S., Bøtter-Jensen, L., Lang, A., 2001. Equivalent dose estimation using a single aliquot of polymineral fine grains. Radiat. Meas. 33, 73–94.
Bekiari, V., Avramidis, P., 2014. Data quality in water analysis: validation of combustion-infrared and combustion-chemiluminescence methods for the simultaneous determination of Total Organic Carbon (TOC) and Total Nitrogen (TN). Int. J. Environ. Anal. Chem. 94 (1), 65–76.
Bignot, G., 1985. Elements of Micropalaeontology, Microfossils - Their Geological and Palaeobiological Applications. Kluwer, Paris.
Blott, S.J., Pye, K., 2001. Gradistat. A grain size distribution and statistics package for the analysis of unconsolidated sediments. Earth Surf. Process. Landf. 26, 1237–1248.
Bronk Ramsey, C., 2009. Bayesian analysis of radiocarbon dates. Radiocarbon 51, 337–360.
Brückner, H., 2005. Holocene shoreline displacements and their consequences for human societies: the example of Ephesus in western Turkey. Z. Geomorphol. 137, 11–22.
Brückner, H., Müllenhoff, M., Handl, M., van der Borg, K., 2002. Holocene landscape evolution of the Büyük Menderes alluvial plain in the environs of Myous and Priene (Western Anatolia, Turkey). Z. Geomorphol. 127, 47–65.
Brückner, H., Vött, A., Schriever, M., Handl, M., 2005. Holocene delta progradation in the eastern Mediterranean—case studies in their historical context. Méditerranée 104, 95–106.
Brückner, H., Kelterbaum, D., Marunchak, O., Porotov, A., Vött, A., 2010. The Holocene sea level story since 7500 BP - lessons from the Eastern Mediterranean, the Black and the Azov Seas. Quat. Int. 225, 160–177.
Bruins, H.J., Alexander, J., Gillivray, Mac, Synolakis, C.E., Benjamini, C., Keller, J., Kisch, H.J., Klügel, A., van der Plicht, J., 2008. Geoarchaeological tsunami deposits at Palaikastro (Crete) and the Late Minoan IA eruption of Santorini. J. Archaeol. Sci. 35, 191–212.
Darlas, A., 1999. Palaeolithic research in western Achaea. In: Bailey, G.N., Adam, E., Panagopoulou, Perlès, C., Zachos, K. (Eds.), The Palaeolithic Archaeology of Greece and Adjacent Areas 303–310 (London).
Davis, R.A., Fitzgerald, D.M., 2004. Beaches and Coasts. Blackwell Science Ltd., Oxford.
Debenay, J.P., Guillou, J.J., Redois, F., Geslin, E., 2000. Distribution trends of foraminiferal assemblages in paralic environments: a base for using foraminifera as early warning indicators of anthropic stress. In: Martin, R. (Ed.), Environmental Micropaleontology. Kluwer Academic/Plenum Publishing Corporation, pp. 39–67.
DIN EN 15936, 2009. Soil, Sludge, Waste and Treated Biowaste - Determination of Total Organic Carbon (TOC) by Dry Combustion.
Evelpidou, N., Pavlopoulos, K., Vassilopoulos, A., Triantaphyllou, Vouvalidis, K., Syrides, G., 2010. Yria (western Naxos Island, Greece): sea level changes in upper Holocene and palaeogeographical reconstruction. Geodin. Acta 23 (5–6), 233–240.
Finné, M., Holmgren, K., Sundqvist, H.S., Weiberg, E., Lindblom, M., 2011. Climate in the eastern Mediterranean regions, during the past 6000 years - a review. J. Archaeol. Sci. 38, 3153–3173.
Folk, R.I., 1974. Petrology of Sedimentary Rocks. Hamphill, Austin, Texas.
Fouache, E., Pavlopoulos, K., 2005. Sea level changes in eastern Mediterranean during the Holocene. Indicators and human impacts. Z. Geomorphol. 137, 193.
Fouache, É., Pavlopoulos, K., Fanning, P., 2010. Geomorphology and geoarchaeology: Cross-contribution. Geodin. Acta 23 (5-6), 207–208.
Frenzel, P., Boomer, I., 2005. The use of ostracods from marginal marine, brackish waters as bioindicators of modern and quaternary environmental change. Palaeogeogr. Palaeoclimatol. Palaeoecol. 225, 68–92.
Frenzel, P., Keyser, D., Viehberg, F.A., 2010. An Illustrated Key and (Palaeo)ecological Primer for Postglacial to Recent Ostracoda (Crustacea) of the Baltic Sea. http://dx.doi.org/10.1111/j.1502-3885.2009.00135.x. (online supplement).
Ghilardi, M., Psomiadis, D., Cordier, S., Delanghe-Sabatier, D., Demory, F., Hamidi, F., Paraschou, T., Dotsika, E., Fouache, E., 2012. The impact of rapid early- to mid-Holocene palaeoenvironmental changes on Neolithic settlement at Nea Nikomideia, Thessaloniki Plain, Greece. Quat. Int. 266, 47–61.
Ghillardi, M., Colleu, M., Pavlopoulos, K., Fachard, S., Psomiadis, D., Rochette, P., Demory, F., Knodell, A., Triantaphyllou, M., Delanghe-Sabatier, D., Bicket, A., Fleury, J., 2013. Geoarchaeology of ancient Aulis (Boeotia, Central Greece): human occupation and Holocene landscape changes. J. Archaeol. Sci. 40, 2071–2083.
Gouma, M., van Wijngaarden, G.J., Soetens, S., 2011. Assessing the effects of geomorphological processes on archaeological densities: a GIS case study on Zakynthos Island, Greece. J. Archaeol. Sci. 38, 2714–2725.
Grigorovich, I.A., Mills, E.L., Richards, C.B., Breneman, D., Ciborowski, J.J.H., 2005. European valve snail *Valvata piscinalis* (Muller) in the Laurentian Great Lakes basin. J. Great Lakes Res. 31 (2), 135–143.
Guiry, M.D., Guiry, G.M., 2008. World-wide Electronic Publication. National University of Ireland, Galway (Retrieved 2009-02-21).
Gupta, S.N.K., 2003. Modern Foraminifera. Kluwer Academic Publishers, New York, pp. 384.
Haenssler, E., Nadeau, M.J., Vott, A., Unkel, I., 2013. Natural and human induced environmental changes preserved in a Holocene sediment sequence from the Etoliko Lagoon, Greece: new evidence from geochemical proxies. Quat. Int. 308–309, 89–104.
Heip, C.H.R., 1976. The Spatial Pattern of *Cyprideis torosa* (Jones, 1850) (Crustacea: Ostracoda). (in: (1976). IZWO Coll. Rep. 6 (1976). IZWO Collected Reprints, 6: pp. chapter 20).
Hiller, D., 1972. Untersuchungen zur Biologie und zur Okologie limnischer Ostracoden aus des Umgebung von Hamburg. Arch. Hydrobiol. Suppl. 40 (4), 400–497.
van Hinsbergen, D.J.J., Zachariasse, W.J., Wortel, M.J.R., Meulenkamp, J.E., 2005. Underthrusting and exhumation: a comparison between the external Hellenides and the "hot" Cycladic and "cold" South Aegean core complexes (Greece). Tectonics 24, 1–19.
Holmes and Miller, 2006. Aspects of the ecology and population genetics of the bivalve *Corbula gibba*. Mar. Ecol. Prog. Ser. 315, 129–140.
I.G.M.E. - Institute of Geology and Mineral Exploration of Greece, 1980. Geological Map of Zakynthos Island Scale 1:50000.
Jones, C.A., Kaiteris, P., 1983. A vacuum-gasometric technique for rapid and precise analysis of calcium carbonate in sediments and soils. J. Sediment. Res. 53, 655–660.
Karakitsios, V., 2013. Western Greece and Ionian Sea petroleum systems. AAPG Bull. 97, 1567–1595.
Kilenyi, T.I., Whittaker, J.E., 1974. On *Cyprideis torosa*, Stereo Atlas of Ostracode Shells. 2(5). pp. 21–32.
Kissel, C., Laj, C., Muller, C., 1985. Tertiary geodynamical evolution of northwestern Greece: paleomagnetic results. Earth Planet. Sci. Lett. 72, 190–204.
Kokkalas, S., Kamberis, E., Xypolias, P., Sotiropoulos, S., Koukouvelas, I., 2012. Coexistence of thin- and thick-skinned tectonics in Zakynthos area (western Greece): insights from seismic sections and regional seismicity. Tectonophysics 597–598, 73–84.
Kontopoulos, N., Avramidis, P., 2003. A late Holocene record of environmental changes from the Aliki lagoon, Egion, North Peloponnesus, Greece. Quat. Int. 111 (1), 75–90.
Kotthoff, U., Koutsodendris, A., Pross, J., Schmiedl, G., Bornemann, A., Kaul, C., Marino, G., Peyron, O., Schiebel, R., 2011. Impact of Lateglacial cold events on the northern Aegean region reconstructed from marine and terrestrial proxy data. J. Quat. Sci. 26, 86–96.
Kraft, J.C., Aschenbrenner, S.E., Rapp, G., 1977. Paleogeographic reconstructions of coastal Aegean archaeological sites. Science 195, 941–947.
Kraft, J.C., Kayan, I., Erol, O., 1980. Geomorphic reconstructions in the environs of ancient Troy. Science 209, 1191–1208.
Kraft, J.C., Rapp, G.R., Kayan, I., Luce, J.V., 2003. Harbor areas at ancient Troy: sedimentology and geomorphology complement Homer's Iliad. Geology 31, 163–166.
Kraft, J.C., Rapp, G., Gifford, J.A., Aschenbrenner, S.E., 2005. Coastal change and archaeolocical settings in Elis. Hesperia 74 (1), 1–39.
Kraft, J.C., Brückner, H., Kayan, I., Engelmann, H., 2007. The geographies of ancient Ephesus and the Artemision in Anatolia. Geoarchaeology 22, 121–149.
Lagios, E., Sakkas, V., Papadimitriou, P., Parcharidis, I., Damiata, B.N., Chousianitis, K., et al., 2007. Crustal deformation in the Central Ionian Islands (Greece): results from DGPS and DInSAR analyses (1995–2006). Tectonophysics 444, 119–145.
Marriner, N., Morhange, C., 2007. Geoscience of ancient Mediterranean harbours. Earth Sci. Rev. 80, 137–194.
Meisch, C., 2000. Freshwater Ostracoda of Western and Central Europe 2000. Spektrum Akademischer Verlag.
Morhange, C., Marriner, N., 2010. Palaeo-hazards in the coastal Mediterranean: a geoarchaelogical approach. In: Martini, I.P., Chesworth, W. (Eds.), Landascapes and Societies, Dordrecht, pp. 223–334.
Meric, E., Ersou, S., Gormus, M., 2001. Twin forms in recent benthic foraminifera from the northern Aegean Sea and western Black Sea regions (Turkey). Rev. Paléobiol. 20 (1), 69–75.
Müller, G., Gastner, M., 1971. The Karbonat-Bombe a Simple Device for the Determination of the Carbonate Content in Sediments, Soils and Other Materials (N.Jb.Miner.Mh.). 10. pp. 466–469.
Murray, A.S., Wintle, A.G., 2000. Luminescence dating of quartz using an improved single – aliquot regenerative – dose protocol. Radiat. Meas. 32, 57–73.
Papadopoulos, G.A., Gràcia, E., Urgeles, R., Sallares, V., De Martini, P.M., Pantosti, D., González, M., Yalciner, A.C., Mascle, J., Sakellariou, D., Salamon, A., Tinti, S., Karastathis, V., Fokaefs, A., Camerlenghi, A., Novikova, T., Papageorgiou, A., 2014. Historical and pre-historical tsunamis in the Mediterranean and its connected seas: geological signatures, generation mechanisms and coastal impacts. Mar. Geol. 354, 81–109.
Papanikolaou, M.D., Triantaphyllou, M.V., Platzman, E.S., Gibbard, P.L., Mac Niocaill, C., Head, M.J., 2011. A well-established Early–Middle Pleistocene marine sequence on South-east Zakynthos island, western Greece: magneto-biostratigraphic constraints and palaeoclimatic implications. J. Quat. Sci. 26, 523–540.
Papazachos, B., Papazachou, 1997. Earthquake in Greece. Publication Zitis, Thessaloniki.
Papazisimou, S., Bouzinos, A., Christanis, K., Tzedakis, P.C., 2000. The coastal asphalt fen of Keri Zakynthos (Hellas). In: 11th International Peat Congress, pp. 58–59.
Pavlopoulos, K., Kapsimalis, V., Theodorakopoulou, K., Panagiotopoulos, I.P., 2012. Vertical displacement trends in the Aegean coastal zone (NE Mediterranean) during the Holocene assessed by geo-archaeological data. The Holocene 22 (6), 717–728.
Pavlopoulos, K., Fouache, E., Sidiropoulou, M., Triantaphyllou, M., Vouvalidis, K., Syrides, G., Gonnet, A., Greco, E., 2013. Palaeoenvironmental evolution and sea-level changes in the coastal area of NE Lemnos Island (Greece) during the Holocene. Quat. Int. 308–309, 80–88.
Rapp, G., Kraft, J.C., 1994. Holocene coastal change in Greece and Aegean Turkey. In: Kardulias, N. (Ed.), Beyond the Site. Regional Studies in the Aegean Area, Lanham. University Press of America, pp. 23–35.
Reimer, P.J., Bard, E., Bayliss, A., Beck, J.W., Blackwell, P.G., Bronk, Ramsey, C., Buck, C.E., Cheng, H., Edwards, R.L., Friedrich, M., Grootes, P.M., Guilderson, T.P., Haflidason, H., Hajdas, I., Hatté, C., Heaton, T.J., Hoffmann, D.L., Hogg, A.G., Hughen, K.A., Kaiser, K.F., Kromer, B., Manning, S.W., Niu, M., Reimer, R.W., Richards, D.A., Scott, E.M., Southon, J.R., Staff, R.A., Turney, C.S.M., van der Plicht, J., 2013. IntCal13 and Marine13 radiocarbon age calibration curves 0–50,000 years cal BP. Radiocarbon 55, 1869–1887.
Scheffers, A., Kelletat, D., Vött, A., May, S.M., Scheffers, S., 2008. Late Holocene tsunami traces on the western and southern coastlines of the Peloponnesus (Greece). Earth Planet. Sci. Lett. 269, 271–279.
Shumilovskikh, L.S., Marret, F., Fleitmann, D., Arz, H.W., Nowaczyk, N., Behling, H., 2013. Eemian and Holocene sea-surface conditions in the southern Black Sea:

organic-walled dinoflagellate cyst record from core 22-GC3. Mar. Micropaleontol. 101, 146–160.
Siani, G., Paterne, M., Arnold, M., Bard, E., Métivier, B., Tisnerat, N., Bassinot, F., 2000. Radiocarbon reservoir ages in the Mediterranean Sea and Black Sea. Radiocarbon 42, 271–280.
Stanley, D.J., Warne, A.G., 1994. Worldwide initiation of Holocene deltas by deceleration of sea-level rise. Science 265, 228–231.
Taraschewski, H., Paperna, I., 1981. Distribution of the snail *Pirenella conica* in Sinai and Israel and its infection by heterophydae and other trematodes. Mar. Ecol. Prog. Ser. 5, 193–205.
Tendürüs, M., van Wijngaarden, G.J., Kars, H., 2010. Long-term effect of seismic activities on archaeological remains: a test study from Zakynthos, Greece. In: Sintubin, M., Stewart, I.S., Niemi, T.M., Altunel, E. (Eds.), Ancient Earthquakes: Geological Society of America Special Paper 471. pp. 145–156.
Torres, T., Ortiz, J.E., Soler, V., Reyes, E., Delgado, A., Valle, M., Llamas, J.F., Cobos, R., Julla, R., Badal, E., Garcia de la Morena, M., Garcia-Martinez, M.J., Fernandez-Gianottis, J., Calvo, J.P., Cortes, A., 2003. Pleistocene lacustrine basin of the east domain of Guadix-Baza Basin (Granada, Spain): sedimentology, chronostratigraphy and palaeoenvironment. In: Valero-Graces, B. (Ed.), Limnogeology in Spain: A Tribute to Kerry Kelts. CSIC, Madrid.
Underhill, J., 1989. Late Cenozoic deformation of the Hellenide foreland, western Greece. Geol. Soc. Am. Bull. 101, 613–634.
Underhill, J.R., 2009. Relocating Odysseus' homeland. Nat. Geosci. 2, 455–458.
Van Wijngaarden, G.J., Kourtessi-Philippakis, G., Pieters, N., 2013. New archaeological sites and finds on Zakynthos. Pharos. J. Netherlands Inst. Athens 19 (1), 127–159.
Verleye, T., Mertens, K., Louwye, S., 2009. Holocene salinity changes in the southwestern Black Sea: a reconstruction based on dinoflagellate cysts. Palynology 33, 77–100.
Vött, A., 2007. Relative sea level changes and regional tectonic evolution of seven coastal areas in NW Greece since the mid-Holocene. Quat. Sci. Rev. 26, 894–919.
Vött, A., Kelletat, D., 2015. Holocene palaeotsunami landfalls and neotectonic dynamics in the western and southern Peloponnese (Greece). Z. Geomorphol. 59 (4), 1–5.
Vött, A., Schriever, A., Handl, M., Brückner, H., 2007. Holocene palaeogeographies of the central Acheloos River delta (NW Greece) in the vicinity of the ancient seaport Oiniadai. Geodin. Acta 20, 241–256.
Vött, A., Brückner, H., Brockmüller, S., Handl, M., May, S.M., Gaki-Papanastassiou, K., Herd, R., Lang, F., Maroukian, H., Nelle, O., Papanastasiou, D., 2009. Traces of Holocene tsunamis across the sound of Lefkada, NW Greece. Glob. Planet. Chang. 66, 112–128.
Vött, A., Lang, F., Brückner, H., Gaki-Papanastassiou, K., Maroukian, H., Papanastassiou, D., Giannikos, A., Hadler, H., Handl, M., Ntageretzis, K., Willershäuser, T., Zander, A., 2011. Sedimentological and geoarchaeological evidence of multiple tsunamigenic imprint on the Bay of Palairos-Pogonia (Akarnania, NW Greece). Quat. Int. 242, 213–239.
Weiberg, E., Unkel, I., Kouli, K., Holmgren, K., Avramidis, P., Bonnier, A., Dibble, F., Finne, M., Izdebski, A., Katrantsiotis, Ch., Stocker, S.R., Andwinge, M., Baika, K., Boyd, M., Heymann, Ch., 2016. The socio-environmental history of the Peloponnese during the Holocene: towards an integrated understanding of the past. Quat. Sci. Rev. 136, 40–65.
WoRMS Editorial Board, 2015. World Register of Marine Species. (Available from http://www.marinespecies.org at VLIZ. Accessed 2016-02-3).
Zelilidis, A., Kontopoulos, N., Avramidis, P., Piper, D.J.W., 1998. Tectonic and sedimentological evolution of the Pliocene–Quaternary basins of Zakynthos, Greece: case study of the transition from compressional to extensional tectonics. Basin Res. 10, 393–408.
Krzymińska, J., Namiotko, T., 2012. Late Glacial and Holocene ostracoda of the Gulf of Gdańsk, the Baltic Sea, Poland. Int. Rev. Hydrobiol. 97 (4), 301–313.